Appl. Phys. A 91, 323–326 (2008)
DOI: 10.1007/s00339-008-4406-5

Applied Physics A
Materials Science & Processing

WANNENG YE[1]
CHAOJING LU[1,2]✉
YAJUN QI[2]
XIAOLIN LIU[2]
STEPHAN SENZ[3]
SUNG KYUN LEE[3]
DIETRICH HESSE[3]

Sol–gel derived ferroelectric $Bi_{3.15}Nd_{0.85}Ti_3O_{12}$ thin films of predominant 100/010/119 orientation deposited both on Nb-doped $(011)SrTiO_3$ and on $(011)SrRuO_3/(011)SrTiO_3$

[1] Laboratory of Fiber Materials and Modern Textile, The Growing Base for State Key Laboratory, Qingdao University, Qingdao 266071, P.R. China
[2] Department of Materials Science and Engineering, Hubei University, Wuhan 430062, P.R. China
[3] Max Planck Institute of Microstructure Physics, Weinberg 2, 06120 Halle, Germany

Received: 5 December 2007/Accepted: 3 January 2008
Published online: 16 February 2008 • © Springer-Verlag 2008

ABSTRACT Ferroelectric $Bi_{3.15}Nd_{0.85}Ti_3O_{12}$ (BNdT) thin films of predominant 100/010/119 orientation were grown through a cheap and simple sol–gel process both on Nb-doped $(011)SrTiO_3$ and on $(011)SrRuO_3/(011)SrTiO_3$. Using rapid heating rates during crystallization, films containing 28% (100)/(010)-oriented grains plus 19% (119)-oriented grains were obtained on $SrRuO_3/SrTiO_3$, while 30% (100)/(010)- and 18% (119)-oriented grains were obtained on $Nb:SrTiO_3$. The films consist of columnar grains and 90° *a*–*b* domains exist in large BNdT grains. The BNdT thin films exhibit excellent ferroelectric and dielectric properties with a remanent polarization $2P_r = 39.2\,\mu C/cm^2$ and a dielectric constant $\varepsilon_r = 184.5$.

PACS 77.80.Fm; 77.80.Dj; 68.60.Wm; 68.55.Jk; 68.37.Lp

1 Introduction

Ferroelectric thin films have been widely investigated in view of their applications in non-volatile memories, piezoelectric microactuators and resonators. Rare-earth-element-substituted $Bi_4Ti_3O_{12}$ films are promising due to their fatigue endurance on Pt electrodes [1, 2]. $Bi_{3.25}La_{0.75}Ti_3O_{12}$ and $Bi_{3.15}Nd_{0.85}Ti_3O_{12}$ (BNdT) films have received attention for their large remanent polarization P_r [3–11]. $Bi_4Ti_3O_{12}$ is monoclinic with the space group $B1a1$ but can be considered pseudo-orthorhombic with $a = 0.545\,nm$, $b = 0.541\,nm$ and $c = 3.283\,nm$. For non-substituted $Bi_4Ti_3O_{12}$ single crystals, the major component of spontaneous polarization (P_s) lies along the *a* axis ($\approx 50\,\mu C/cm^2$); the component along the *c* axis is very small ($\approx 4\,\mu C/cm^2$) [12]. This ferroelectric anisotropy requires the growth of non-*c*-axis-oriented films to achieve large P_r values in planar-type capacitors. Thin films having a larger fraction of *a*-axis- (or near-*a*-axis)-oriented grains should exhibit better ferro-, piezo- and dielectric properties [13]. However, such films tend to grow with the *c* axis perpendicular to the film plane.

✉ Fax: +86-532-85955977, E-mail: cjlu@qdu.edu.cn

Recently, the growth of rare-earth-element-substituted $Bi_4Ti_3O_{12}$ films with *a*/*b*-axes orientation [3, 4, 14–16] and with (104)/(014) orientation [5, 8, 10, 11, 15–18] by the elaborative pulsed laser deposition (PLD) or metal–organic chemical vapor deposition (MOCVD) methods was reported and all this work confirmed the crucial role of the crystallographic orientation. Unfortunately, there are few reports on such oriented films grown by chemical solution deposition (CSD) [7, 19–22]. We previously reported a cheap and simple route to grow BNdT films with predominant *a*/*b*-axes orientation on $(111)Pt/Ti/SiO_2/Si$ through the sol–gel method and on the large anisotropy of their ferro-, piezo- and dielectric properties [7, 22]. The present letter reports predominantly *a*/*b*-axes- and (119)-oriented BNdT thin films grown both on Nb-doped $(011)SrTiO_3$ and on $SrRuO_3$-buffered $(011)SrTiO_3$ substrates, quantifies the amount of the predominant orientation, considers their microstructure and characterizes their electrical properties. The results are summarized in Table 1.

2 Experimental procedure

The BNdT thin films were deposited on $Nb:SrTiO_3$ (011) and on $SrRuO_3/(011)SrTiO_3$ single-crystal substrates using a sol–gel process. Appropriate amounts of $Bi(NO_3)_3 \cdot 5H_2O$, $Nd(CH_3COO)_3$ and $Ti(OC_4H_9)_4$ were dissolved in an acidic solution. 4 mol % excess bismuth nitrate was added to compensate for the Bi loss during annealing. The as-deposited films were pyrolyzed at 450 °C in air, followed by annealing at 750 °C in flowing oxygen. The heating rate was about 80 °C/s. Each single-annealed layer is ∼ 15-nm thick. The deposition–crystallization cycles were repeated many times to obtain the desired thickness. Pt top electrodes of 0.24-mm^2 size were deposited by sputtering using a shadow mask. Ferroelectric measurements were performed on a TF Analyzer 2000 ferroelectric tester (aixAcct) at a frequency of 1 kHz, and dielectric measurements on a Hewlett-Packard 4194A low-frequency impedance analyzer using an ac signal of 1 MHz and 10-mV amplitude.

3 Results and discussion

X-ray diffraction (XRD) was performed on a Philips X'Pert MRD four-circle diffractometer using Cu K_α radiation. Figure 1 shows a XRD θ–2θ scan of a 475-nm-

Substrate	Film thickness	Preferred orientation	$2P_r$ ($\mu C/cm^2$)	E_c (kV/cm)
$SrRuO_3/SrTiO_3(011)$	475 nm	28% (100)/(010) + 19% (119)	39.3	197
$Nb:SrTiO_3(011)$	430 nm	30% (100)/(010) + 18% (119)	26.2	153

TABLE 1 Comparison of the preferred orientations and electrical properties for the BNdT thin films grown on different substrates

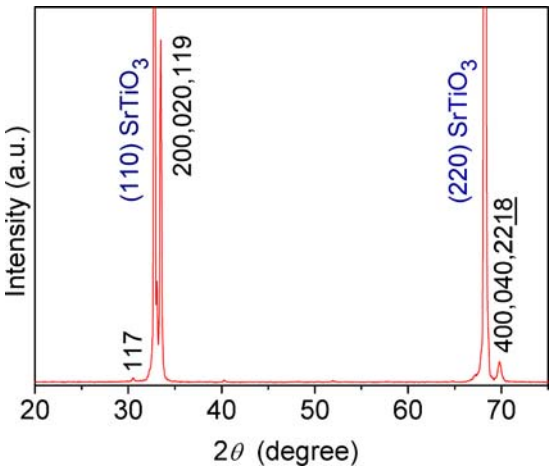

FIGURE 1 XRD θ–2θ scan of a BNdT thin film deposited on $(011)SrRuO_3/(011)SrTiO_3$. The $SrRuO_3$ layer is so thin (~ 20 nm) that no diffraction peak is detected for it

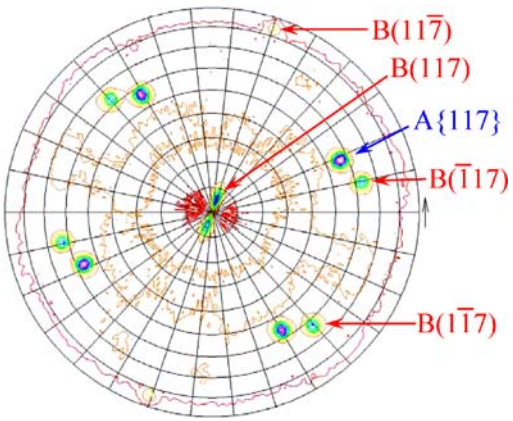

FIGURE 2 X-ray pole figure recorded from the BNdT (117) reflection of the films on $(011)SrRuO_3/(011)SrTiO_3$. Peaks originating from (100)/(010)- and (119)-oriented grains in the BNdT films are denoted 'A' and 'B', respectively. The center and rim of the pole figure correspond to $\psi = 0°$ and 90°, respectively

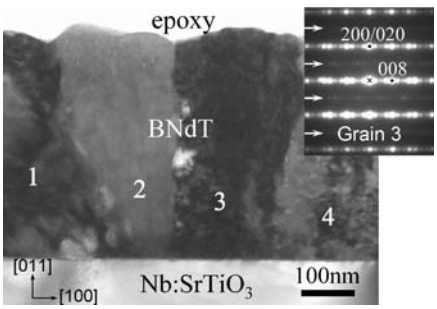

FIGURE 3 Cross-sectional TEM image of a BNdT film grown on $Nb:SrTiO_3(011)$. The *inset* is a SAED pattern of the columnar grain 3 in the [100]/[010] direction

thick BNdT film deposited on $(011)SrTiO_3/(011)SrRuO_3$. The peaks of the film are indexed according to the standard powder diffraction data of $Bi_{3.6}Nd_{0.4}Ti_3O_{12}$ [23]. In the standard data, the 117 reflection is the strongest peak. In Fig. 1, the 200/020/119 peak is much stronger than the 117 peak, suggesting that the film is predominantly 100/010- and 119-oriented.

The crystallographic orientations of the BNdT film were confirmed by the X-ray pole figure recorded from the BNdT (117) reflection; see Fig. 2. The pole figure consists of two sets of peaks marked with 'A' and 'B', respectively. The major set 'A' appears at $\psi \approx 57°$ and stems from the 100/010-oriented BNdT grains because of the angles $\angle(100):(117) = 56.88°$ and $\angle(010):(117) = 56.7°$, while the minor set 'B' is composed of peaks located at $\psi \approx 7$, 63 and 86° and originates from the 119-oriented grains (cf. the angles $\angle(119) : (117) = 7.16°$, $\angle(119):(\underline{1}17) = 62.58°$, $\angle(119):(\underline{1}1\underline{7}) = 62.89°$ and $\angle(119):(11\underline{7}) = 85.64°$). The background intensities are in the range of 10–70 cps, while the maximum intensity at the peaks $\psi \approx 57°$ is about 6757 cps, indicating a mixture of (100)/(010), (119) and random orientations. According to the pole figure, the volume fraction of the (100)/(010)-oriented grains in the film can be estimated to be around 28% by calculating the following fraction. The numerator of the fraction is the sum of the integral intensity of the four peaks marked with 'A' and that of the background ring with the ψ angle around 56.88°, while its denominator is the integral intensity of the whole pole figure including all the peaks and background. The volume fraction of the 119-oriented grains in the film can be estimated to be around 19% by calculating as follows: The numerator of the fraction is the sum of the integral intensity of the eight peaks marked with 'B' and that of the background rings with the ψ angle around 7.16, 62.58 and 85.64°, while its denominator is the integral intensity of the whole pole figure. In the same way, the texture of the BNdT films on $Nb:SrTiO_3(011)$ was estimated to be $\sim 30\%(100)/(010) + 18\%(119)$; see Table 1.

The microstructure of the BNdT films was investigated using transmission electron microscopy (TEM) on a Tecnai G^2 microscope. Figure 3 shows a cross-sectional TEM image of the 430-nm-thick BNdT films grown on $Nb:SrTiO_3(011)$. The inset is a selected area electron diffraction (SAED) pattern of the columnar grain 3 with a/b-axis orientation. The SAED pattern could result from the [100] zone or from the superposition of [100] and [010] zones, where the [010] zone gives a pattern similar to the inset, however with the weak reflections indicated by arrows missing [24, 25]. One can see from Fig. 3 that the BNdT films consist of large columnar grains penetrating the film thickness. Similar columnar grains were observed in the films deposited on $(011)SrRuO_3/(011)SrTiO_3$.

Given the columnar growth shown by Fig. 3, the crystallographic orientation of the columnar grains will be determined by the nucleation of the crystalline phase from the amorphous one in the regions close to the substrate, during the crystallization anneal. PLD-grown films of the bismuth-layered perovskites tend to grow c-axis-oriented, especially

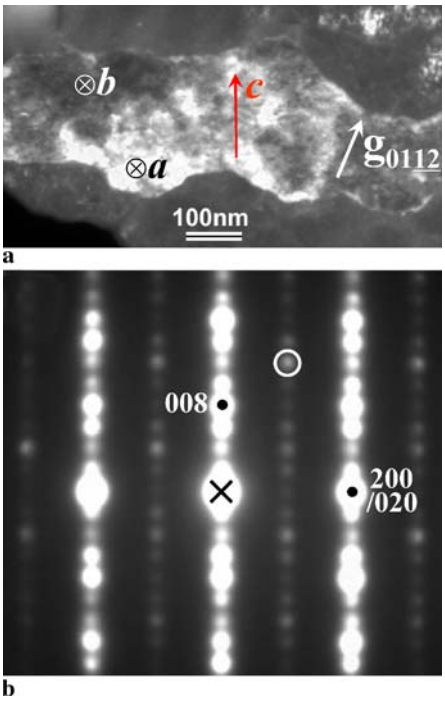

FIGURE 4 (**a**) Plan-view dark-field TEM image (taken under $g = 01\underline{12}$) showing 90° *a–b* domains in a large BNdT grain on Nb:$SrTiO_3$(011), (**b**) SAED pattern of the grain in the [100]/[010] direction

at low growth rates, due to the low interface energy of *c*-axis-oriented films on (100)-plane perovskite substrates, and partially due to the fact that the growth in the *a–b* plane is considerably faster than along the *c* axis. In our case of CSD-grown and crystallization-annealed films on (011)-plane perovskite substrates, a high heating rate for crystallization could be crucial for the nucleation of non-*c*-axis-oriented grains. A large heating rate may result in a rapid increase of thermal stress due to the quickly increasing thermal expansion difference, which certainly will modify the interface energy. Thus, other crystallographic orientations than the *c*-axis orientation may be favored during nucleation in this case.

Figure 4a is a plan-view TEM dark-field image (taken under $g = 01\underline{12}$) of a large BNdT grain on Nb:$SrTiO_3$(011). The SAED pattern, shown in Fig. 4b, results from the superposition of [100] and [010] zones, indicating the *a*/*b*-axis orientation of the grain. 90° *a–b* domains in the grain are visualized as bright–dark contrasts in Fig. 4a. The domain walls are irregular and curved, similar to the case in (001)-oriented $SrBi_2Nb_2O_9$ (SBN) grown on $SrTiO_3$(001) [26]. We observed 90° *a–b* domains frequently in large BNdT grains, seldom in fine grains with dimensions < 80 nm. This fact supports the explanation that 90° *a–b* domains in layered ferroelectric perovskites are formed due to long-range 'interchange' of the *a* and *b* axes (comparable in the length scale [25, 26]).

Figure 5 shows the polarization–electric field (*P–E*) hysteresis loops of the Pt/BNdT/$SrRuO_3$ film capacitors on (011)$SrTiO_3$. The BNdT films have a coercive field E_c of ∼ 197 kV/cm, higher than that (E_c = 108 kV/cm) of the predominantly *a*/*b*-axis-oriented BNdT films on Pt/Ti/SiO_2/Si but lower than that (E_c = 265 kV/cm) of *a*/*b*-axes-oriented $Bi_{3.25}La_{0.75}Ti_3O_{12}$ (BLT) epitaxial films grown on $SrRuO_3$/YSZ/Si [3, 7].The BNdT films of predominant

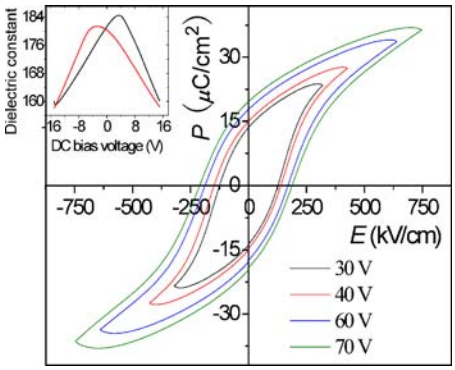

FIGURE 5 *P–E* hysteresis loops of a film capacitor on (011)$SrRuO_3$/(011)$SrTiO_3$. The *inset* shows the dependence of the dielectric constant ε_r on the dc-bias voltage for a BNdT film on Nb:$SrTiO_3$(011)

100/010/119 orientation showed a $2P_r$ of ∼ 39.2 μC/cm² at an applied field of 737 kV/cm. Interestingly, this $2P_r$ value is much higher than that (12 μC/cm²) of (118)-oriented BNdT epitaxial films grown on (011)$SrRuO_3$/(011)$SrTiO_3$ [5], but close to the $2P_r$ value (∼ 39 μC/cm²) of the predominantly *a*/*b*-axis-oriented BNdT films on Pt/Ti/SiO_2/Si [7]. It is, however, lower than that (64 μC/cm²) of *a*/*b*-axis-oriented BLT epitaxial films grown on $SrRuO_3$/YSZ/Si [3].

The inset of Fig. 5 shows the dependence of the dielectric constant ε_r on dc-bias voltage for a BNdT film on Nb:$SrTiO_3$(011). The butterfly-shaped ε_r–*V* curve reflects the ferroelectric behavior of the Pt/BNdT/Nb:$SrTiO_3$ capacitors, like the *P–E* hysteresis loops of Fig. 5. Because of the non-symmetrical electrodes, the two dielectric peaks have different maximum ε_r values of 181.4 and 184.5. The two peaks are located at the voltages of ±3.4 V (39.5 kV/cm), corresponding to two coercive voltages. The voltage value is much less than the apparent coercive voltage obtained from the *P–E* loops. The difference may be due to the fact that the dc bias voltage ramp rate was much slower than that of the stimulus voltage in hysteresis measurement.

4 Conclusions

In summary, ferroelectric BNdT thin films with predominant (100)/(010)/(119) orientation were deposited both on Nb:$SrTiO_3$(011) and on (011)$SrRuO_3$/$SrTiO_3$(011) through a cheap and simple sol–gel process. The films exhibit excellent ferroelectric properties with a $2P_r$ value of 39.2 μC/cm². Heating rapidly for crystallization is crucial for the nucleation of non-*c*-axis-oriented grains. Using a very thin single-annealed layer is favorable to increase the volume fraction of the non-*c*-axis-oriented grains.

ACKNOWLEDGEMENTS This work was supported by the Research Foundation of Ph.D-degree-conferred subject in University (20070512002), the Program for New Century Excellent Talents (NCET) in University and the Program for Excellent Young Scientists in Wuhan City, China; work at MPI Halle supported by DFG via SFB 418 and FOR 404.

REFERENCES

1 C.A.P. de Araujo, J.D. Cuchiaro, L.D. McMillan, M.C. Scott, J.F. Scott, Nature (London) **374**, 627 (1995)
2 B.H. Park, B.S. Kang, S.D. Bu, T.W. Noh, J. Lee, W. Jo, Nature (London) **401**, 682 (1999)

3 H.N. Lee, D. Hesse, N. Zakharov, U. Gösele, Science **296**, 2006 (2002)
4 T. Watanabe, T. Kojima, H. Uchida, I. Okada, H. Funakubo, Japan. J. Appl. Phys. **43**, L309 (2004)
5 A. Garg, Z.H. Barber, M. Dawber, J.F. Scott, A. Snedden, P. Lightfoot, Appl. Phys. Lett. **83**, 2414 (2003)
6 J.H. Li, Y. Qiao, X.L. Liu, C.J. Nie, C.J. Lu, Z.X. Xu, S.M. Wang, N.X. Zhang, D. Xie, H.C. Yu, J.Q. Li, Appl. Phys. Lett. **85**, 3193 (2004)
7 C.J. Lu, Y. Qiao, Y.J. Qi, X.Q. Chen, J.S. Zhu, Appl. Phys. Lett. **87**, 222 901 (2005)
8 S.K. Lee, D. Hesse, U. Gösele, Appl. Phys. Lett. **88**, 062 909 (2006)
9 U. Chon, H.M. Jang, M.G. Kim, C.H. Chang, Phys. Rev. Lett. **89**, 087 601 (2002)
10 S.K. Lee, D. Hesse, U. Gösele, J. Appl. Phys. **100**, 044 108 (2006)
11 D. Hesse, S.K. Lee, U. Gösele, Phys. Stat. Solidi A **202**, 2287 (2005)
12 S.E. Cummins, L.E. Cross, J. Appl. Phys. **39**, 2268 (1968)
13 C. Harnagea, A. Pignolet, M. Alexe, D. Hesse, U. Gösele, Appl. Phys. A **70**, 261 (2000)
14 H. Matsuda, S. Ito, T. Iijima, Appl. Phys. Lett. **85**, 1220 (2004)
15 T. Watanabe, H. Funakubo, K. Saito, T. Suzuki, M. Fujimoto, M. Osada, Y. Noguchi, M. Miyayama, Appl. Phys. Lett. **81**, 1660 (2002)
16 T. Watanabe, H. Funakubo, Japan. J. Appl. Phys. **44**, 1337 (2005)
17 T. Kojima, T. Sakai, T. Watanabe, H. Funakubo, K. Saito, M. Osada, Appl. Phys. Lett. **80**, 2746 (2002)
18 H.N. Lee, D. Hesse, Appl. Phys. Lett. **80**, 1040 (2002)
19 R. Iijima, Appl. Phys. Lett. **79**, 2240 (2001)
20 G.D. Hu, I.H. Wilson, J.B. Xu, W.Y. Cheung, S.P. Wong, H.K. Wong, Appl. Phys. Lett. **74**, 1221 (1999)
21 G. Asayama, J. Lettieri, M.A. Zurbuchen, Y. Jia, S. Trolier-McKinstry, D.G. Schlom, S.K. Streiffer, J.P. Maria, S.D. Bu, C.B. Eom, Appl. Phys. Lett. **80**, 2371 (2002)
22 C.J. Lu, X.L. Liu, X.Q. Chen, C.J. Nie, G. Le Rhun, S. Senz, D. Hesse, Appl. Phys. Lett. **89**, 062 905 (2006)
23 H. McMurdie, M. Morris, E. Evans, B. Paretzkin, W. Wong-Ng, C. Hubbard, Powder Diffract. **1**, 84 (1986)
24 M.W. Chu, S.K. Lee, D. Hesse, U. Gösele, Appl. Phys. Lett. **85**, 2029 (2004)
25 M.W. Chu, M.T. Caldes, L. Brohan, M. Ganne, A.M. Marie, O. Joubert, Y. Piffard, Chem. Mater. **16**, 31 (2004)
26 M.A. Zurbuchen, G. Asayama, D.G. Schlom, S.K. Streiffer, Phys. Rev. Lett. **88**, 107 601 (2002); the spontaneous polarization of SBN is entirely along the *a* direction